

# รายงานวิจัยฉบับสมบูรณ์

การประยุกต์ใช้คอมพิวเตอร์ช่วยวิศวกรรมเอนไซม์ ฟรุกโตซิลทรานเฟอเรสตระกูล 32 เพื่อใช้ในการสังเคราะห์ ฟรุกโตโอลิโกแซคคาไรด์

โดย ผู้ช่วยศาสตราจารย์ ดร.จิตระยุทธ์ จิตอ่อนน้อม

# สัญญาเลขที่ TRG5880241

# รายงานวิจัยฉบับสมบูรณ์

การประยุกต์ใช้คอมพิวเตอร์ช่วยวิศวกรรมเอนไซม์ ฟรุกโตซิลทรานเฟอเรสตระกูล 32 เพื่อใช้ในการสังเคราะห์ ฟรุกโตโอลิโกแซคคาไรด์

ผู้ช่วยศาสตราจารย์ ดร.จิตระยุทธ์ จิตอ่อนน้อม คณะวิทยาศาสตร์ มหาวิทยาลัยพะเยา

สนับสนุนโดยสำนักงานกองทุนสนับสนุนการวิจัย

# บทคัดย่อ

รหัสโครงการ: TRG5880241

ชื่อโครงการ: การประยุกต์ใช้คอมพิวเตอร์ช่วยวิศวกรรมเอนไซม์ฟรุกโตซิลทรานเฟอเรส

ตระกูล 32 เพื่อใช้ในการสังเคราะห์ฟรุกโตโอลิโกแซคคาไรด์

ชื่อนักวิจัย: ผู้ช่วยศาสตราจารย์ ดร.จิตระยุทธ์ จิตอ่อนน้อม มหาวิทยาลัยพะเยา

**E-mail:** jitrayut.018@gmail.com

ระ<mark>ยะเวลา:</mark> 1 กรกฎาคม พ.ศ. 2558 ถึง 30 มิถุนายน พ.ศ. 2560

เอนไซม์ฟรุกโตซิลทรานเฟอเรสมีความจำเพาะเจาะจงต่อการย่อยน้ำตาลซูโครสที่ ตำแหน่งพันธะไกลโคซิดิกชนิดเบต้า (2→1) โดยปลดปล่อยน้ำตาลกลูโคส พร้อมกับย้ายหมู่ ฟรุกโตสเพื่อเข้าจับกับโมเลกุลที่เป็นตัวรับ เอนไซม์ชนิดนี้มีศักยภาพในการผลิตฟรุกโตโอลิโก แซคคาไรด์ ซึ่งได้รับความสนใจจากอุตสาหกรรม ปัจจุบันถึงแม้ว่าเอนไซม์ประเภทนี้ได้รับ การศึกษาอย่างมาก แต่กลไกการเกิดปฏิกิริยาของเอนไซม์ยังไม่เป็นที่เข้าใจเด่นชัดนัก โดยเฉพาะข้อมูลระดับโมเลกุลเกี่ยวกับการสังเคราะห์น้ำตาลฟรุกโตโอลิโกแซคคาไรด์ด้วย เอนไซม์จากน้ำตาลซูโครส ดังนั้นในโครงการวิจัยนี้ คณะผู้วิจัยจึงได้ประยุกต์ใช้ระเบียบวิธี ผสมผสานกลศาสตร์ควอนตัมและกลศาสตร์โมเลกุล เพื่อศึกษากระบวนการสลายน้ำตาลและ กระบวนการย้ายหมู่ฟรุกโตสของเอนไซม์ฟรุกโตซิลทรานเฟอเรสจากยีสต์ (A. japonicus) โดยมี น้ำตาลซูโครสทำหน้าที่เป็นตัวให้และตัวรับระหว่างเกิดปฏิกิริยา ผลการศึกษาพบว่าปฏิกิริยา ขั้นตอนแรกของกระบวนการฟรุกโตซิเลชันเป็นขั้นกำหนดอัตรา โดยมีค่าพลังงานกระตุ้นเท่ากับ 15.7 กิโลแคลอรีต่อโมล ที่ระดับการคำนวณ SCC-DFTB/CHARMM22 สำหรับปฏิกิริยาขั้นตอน ที่สองนั้น คณะผู้วิจัยสามารถอธิบายกระบวนการย่อยสลายและกระบวนการย้ายหมู่ฟรุกโตสได้ เป็นครั้งแรก โดยพบว่าทั้งสองกระบวนการเกิดขึ้นแบบแข่งขันกัน โดยมีค่าพลังงานกระตุ้น ใกล้เคียงกัน (~10 กิโลแคลอรีต่อโมล) ในแต่ละขั้นตอนของปฏิกิริยานั้น จะพบว่ามีโครงสร้าง ทรานซิชันชนิดออกโซคาร์บอเนียมเกิดขึ้นที่น้ำตาลฟรุกโตสตำแหน่ง –1 และมีรูปร่างชนิด C4'endo ผลการจำลองพลวัติเชิงโมเลกุลของโครงสร้างเชิงซ้อนของน้ำตาลซูโครสกับเอนไซม์ชนิด ไม่กลายพันธุ์ กับชนิดกลายพันธุ์ D191A ชี้ให้เห็นว่า กรดแอสพาร์ติกลำดับที่ 191 มีหน้าที่ เกี่ยวข้องกับการคงรูปร่างของน้ำตาลให้เหมาะสมต่อการเร่งปฏิกิริยาของเอนไซม์ นอกจากนี้ คณะผู้วิจัยยังพบรูปแบบอันตรกิริยาที่สำคัญ คือ Asp119···nucleophile···1-OH (substrate) ซึ่ง ใช้เป็นตัวบ่งชี้ถึงความเป็นไปได้ในการเกิดสารมัธยันตร์ของปฏิกิริยา โดยสรุปโครงการวิจัยนี้ สามารถอธิบายกระบวนการสังเคราะห์น้ำตาลฟรุกโตโอลิโกแซคคาไรด์ในระดับโมเลกุลได้เป็น ครั้งแรก โดยความรู้ที่ได้นั้นสามารถนำไปประยุกต์ใช้กับเอนไซม์ชนิดอื่นๆ ที่สังเคราะห์น้ำตาล หนิดเดียวกันได้

คำหลัก: ระเบียบวิธีผสมผสานกลศาสตร์ควอนตัมและกลศาสตร์โมเลกุล; เอนไซม์ฟรุกโต ซิลทรานเฟอเรส; ปฏิกิริยาทรานไกลโคสิเลชัน; พรีไบโอติก; SCC-DFTB

#### Abstract

Project code: TRG5880241

Title: Computer-aided engineering family GH32 fructosyltransferase for

use in fructooligosaccharide synthesis

Investigator: Assistant Professor Dr. Jitrayut Jitonnom, University of Phayao

**E-mail:** jitrayut.018@gmail.com

Project period: 1 July 2015 to 30 June 2017

Fructosyltransferases (FT) act on sucrose by cleaving the  $\beta$ -(2 $\longrightarrow$ 4) linkage, releasing glucose, and then transferring the fructosyl group to an acceptor molecule. This enzyme is capable of producing prebiotic fructooligosaccharides (FOS) that are of industrial interest. While several FOS-synthesizing enzymes FTs have been investigated, their catalytic mechanism is not fully understood yet, especially the molecular details of how enzymatically synthesized FOS is obtained from sucrose. In this research project, we present a comparative QM/MM investigation on the hydrolysis and transfructosylation reactions catalyzed by a yeast FT from A. japonicus using sucrose as donor and acceptor molecule. It is shown that the fructosylation of the substrate is the rate-determining step of the whole catalytic cycle with an energy barrier of 15.7 kcal mol<sup>-1</sup> [at SCC-DFTB/CHARMM22], in good agreement with the published experimental data. For the defructosylation, both the hydrolysis and transfructosylation of the fructosyl-enzyme intermediate were explored and the two reactions seem to be competitive with similar energy barriers (~10 kcal mol<sup>-1</sup>). For all studied reaction steps, the oxocarbonium transition state was observed on the fructosyl ring bound in the -1 position, having a C4'-endo conformation. Based on the SCC-DFTB/MM simulations of sucrose complex in wildtype and D191A mutant, Asp191 is shown to be responsible for the productive sugar conformation (at subsite -1) required for catalysis. An interaction pattern, Asp119...nucleophile...1-OH (substrate), is proposed to determine the feasibility of the formation of the intermediate. This is the first computational study for understanding the FOS synthesis process, which can be applicable to other related FOS-synthesizing enzymes.

Keyword: QM/MM; fructosyltransferase; transglycosylation; prebiotic; SCC-DFTB

### 1.1 Introduction to the research problem and its significance

Transglycosylation (TG) activity is a property of some glycoside hydrolases (GHs, glycosidases) with which new glycosidic bonds are introduced between donor and acceptor sugar molecules. This special property could potentially generate longer chain oligosaccharides. It can be employed for production of useful oligosaccharides with valuable properties, for example, antitumor properties, and ability to control cell growth, antioxidant effects, and the capacity to trigger defense systems in plants. At the present, only a few GHs have been reported to show such TG activity with a limited number of a highly efficient TG in GHs.

Family GH32 fructosyltransferases (FTs) catalyze both hydrolysis and transglycosylation (TG) reactions. The TG by these enzymes has received much attention for prebiotic fructooligosaccharides (FOS) that are of industrial interest. While several FOS-synthesizing enzymes FTs from various organisms have been characterized and modified for TG activity by mutagenesis, efficient TG has as yet been accomplished with only partial success. In addition, what determines the balance between TG and hydrolysis (TG/hydrolysis ratio) remains a key unresolved question until now.

Computational design of a new enzyme (e.g., by mutations) with an expectation of 'new' activity/function is more reasonable and rational approach for prediction. It can be used to complement the experiment and/or to guide future experimental design. Hybrid quantum mechanics/molecular mechanics (QM/MM) methods are computational tools that are popular for the study of enzyme catalysis at the molecular level. These QM/MM methods have been proved to provide not only the atomistic insights into a fundamental basis of enzyme catalysis, but also very useful information for future biocatalyst design and enzyme engineering.

#### 2. Objectives

- 2.1 To establish theoretical models that could account for the reaction rate of both hydrolysis and TG observed experimentally in wildtype and mutants
- 2.2 To identify the underlying structural, thermodynamics and kinetic factors that might govern the TG activity in GH32 FT from *A. japonicas*
- 2.3 To establish a QM/MM approach for future rational design of engineered glycosidase with significant TG activity

#### 3. Methodology

### 3.1 Modeling wildtype and mutant FT with FOS bound

- 3.1.1 Searching for the ES crystal structure from Protein Databank (PDB) with high X-ray resolution
- 3.1.2 Generating wildtype and mutant structures of FT. Reverting mutation to obtain a wildtype structure (if a mutant X-ray structure)
- 3.1.3 Adding missing hydrogen atoms to the X-ray crystal structure and then minimization
- 3.1.4 Evaluating the refined crystal structure

#### 3.2 Setting up QM/MM

- 3.2.1 Selecting the active site residues and substrate to be treated in QM. This QM treated with SCC-DFTB method is used to describe bond breaking and bond forming in the reaction.
- 3.2.2 The remaining residues (excluding the QM region) including the water molecule is treated molecular mechanically (MM) with CHARMM all-atom force field which is used to describe the interactions of molecule classically.

# 3.3 Simulations of wildtype and mutant FT complex with donor/acceptor substrate

- 3.3.1 The complexes were solvated by a 25 Å radius sphere of TIP3P model waters centered on the anomeric carbon atom
- 3.3.2 QM/MM MD simulations of the enzyme complex were carried out at 300 K

#### 3.4 Modeling hydrolysis and TG reactions with QM/MM energy minimization

- 3.4.1 Finding the suitable reaction coordinate to be used in reaction modeling
- 3.4.2 Calculating the potential energy surface (PES) using adiabatic mapping at [QM/MM(SCC-DFTB:CHARMM)] level.
- 3.4.3 Plotting the PES against the reaction coordinate used
- 3.4.4 Comparing the calculated energy barrier of TG with that of hydrolysis

#### 3.5 Residue analysis

- 3.5.1 The QM/MM interaction energy with and without each selected residue deleted was evaluated and denoted as  $\Delta \textit{E}(\text{QM/MM}_{\text{elec}})$
- 3.5.2 Positive and negative values of  $\Delta E(\text{QM/MM}_{\text{elec}})$  indicate that the residue stabilizes or destabilizes the reacting system, respectively.

# 4. Schedule for the entire project

Research plan  1-6 6-12 12-18 18-24  1. Modeling wildtype and mutant FT with FOS bound - Searching for the ES crystal structure from Protein Databank (PDB) with high X-ray resolution - Generating wildtype and mutant structures of FT. Reverting mutation to obtain a wildtype structure (if a mutant X-ray structure) - Adding missing hydrogen atoms to the X-ray crystal structure and then minimization - Evaluating the refined crystal structure  2. Set up QM/MM for enzyme models - QM region was treated by SCC-DFTB and MM region was treated by CHARMM
bound  - Searching for the ES crystal structure from Protein Databank (PDB) with high X-ray resolution  - Generating wildtype and mutant structures of FT. Reverting mutation to obtain a wildtype structure (if a mutant X-ray structure)  - Adding missing hydrogen atoms to the X-ray crystal structure and then minimization  - Evaluating the refined crystal structure  2. Set up QM/MM for enzyme models  - QM region was treated by SCC-DFTB and MM region was
- Searching for the ES crystal structure from Protein Databank (PDB) with high X-ray resolution - Generating wildtype and mutant structures of FT. Reverting mutation to obtain a wildtype structure (if a mutant X-ray structure) - Adding missing hydrogen atoms to the X-ray crystal structure and then minimization - Evaluating the refined crystal structure  2. Set up QM/MM for enzyme models - QM region was treated by SCC-DFTB and MM region was
Databank (PDB) with high X-ray resolution  - Generating wildtype and mutant structures of FT.  Reverting mutation to obtain a wildtype structure (if a mutant X-ray structure)  - Adding missing hydrogen atoms to the X-ray crystal structure and then minimization  - Evaluating the refined crystal structure  2. Set up QM/MM for enzyme models  - QM region was treated by SCC-DFTB and MM region was
- Generating wildtype and mutant structures of FT.  Reverting mutation to obtain a wildtype structure (if a mutant X-ray structure)  - Adding missing hydrogen atoms to the X-ray crystal structure and then minimization  - Evaluating the refined crystal structure  2. Set up QM/MM for enzyme models  - QM region was treated by SCC-DFTB and MM region was
Reverting mutation to obtain a wildtype structure (if a mutant X-ray structure)  - Adding missing hydrogen atoms to the X-ray crystal structure and then minimization  - Evaluating the refined crystal structure  2. Set up QM/MM for enzyme models  - QM region was treated by SCC-DFTB and MM region was
mutant X-ray structure)  - Adding missing hydrogen atoms to the X-ray crystal structure and then minimization  - Evaluating the refined crystal structure  2. Set up QM/MM for enzyme models  - QM region was treated by SCC-DFTB and MM region was
- Adding missing hydrogen atoms to the X-ray crystal structure and then minimization - Evaluating the refined crystal structure  2. Set up QM/MM for enzyme models - QM region was treated by SCC-DFTB and MM region was
structure and then minimization - Evaluating the refined crystal structure  2. Set up QM/MM for enzyme models - QM region was treated by SCC-DFTB and MM region was
- Evaluating the refined crystal structure  2. Set up QM/MM for enzyme models - QM region was treated by SCC-DFTB and MM region was
2. Set up QM/MM for enzyme models - QM region was treated by SCC-DFTB and MM region was
- QM region was treated by SCC-DFTB and MM region was
treated by CHARMM
3. Simulations of wildtype and mutant FT
complex with donor/acceptor substrate
- Solvating the complexes with TIP3P model waters within 25
Å of the anomeric carbon
- Running QM/MM MD simulations of the enzyme complex at
300 K
4. Modeling hydrolysis and TG reactions with
QM/MM energy minimization
- Finding the suitable reaction coordinate to be used in reaction modeling
- Calculating the potential energy surface (PES) using
adiabatic mapping at [QM/MM(SCC-DFTB:CHARMM) level
- Plotting the PES against the reaction coordinate
- Comparing the calculated energy barrier of TG with that of
hydrolysis
5. Residue analysis
- Calculating the QM/MM interaction energies with and
without each selected residue deleted
- Identifying which residues stabilize or destabilize the
system from the magnitude of $\Delta E$ (QM/MM $_{ ext{elec}}$ ) energies for
each individual residue
6. Comparing the calculated results with
experiment
7 Conclusion and report

#### 2.1 Introduction

Fructooligosaccharides (FOSs) are of increasing interest as "functional sweeteners" because of their health benefits, including non-cariogenicity, low caloric value, and the ability to stimulate the growth of beneficial colonic lactic acid bacteria and to enhance the intestinal immune response <sup>1</sup>. They are also prebiotic substances found in many vegetable or natural foods<sup>2</sup>. Because of low extraction yields of FOSs from natural sources and their limited chemical structures, biocatalytic approaches based on enzyme catalyzed transfructosylation reactions <sup>3</sup> are attractive for the synthesis of welldefined FOSs. Currently, commercially available FOSs for human consumption are exclusively inulin-type prebiotics with  $\beta$ -(2 $\longrightarrow$ 1)-linkages, such as 1-kestose and nystose (see Figure 1); all of which can be produced from sucrose by the action of fructosyltransferase (FT). FTs are found in many plants and microorganisms <sup>4</sup>. Among the studied FOS-synthesizing enzymes, fugal FTs or β-fructofuranosidases have attracted industrial attention for the mass production of FOS. A growing number of fugal FT genes have been extensively characterized with high transfructosylation/hydrolysis ratios over the past few years <sup>3d, 5</sup>. Fugal FTs from *Asperaillus* sp. <sup>4</sup> have been studied extensively along with others from related species, such as Aureobasidium, Penicillium, and Fusarium.

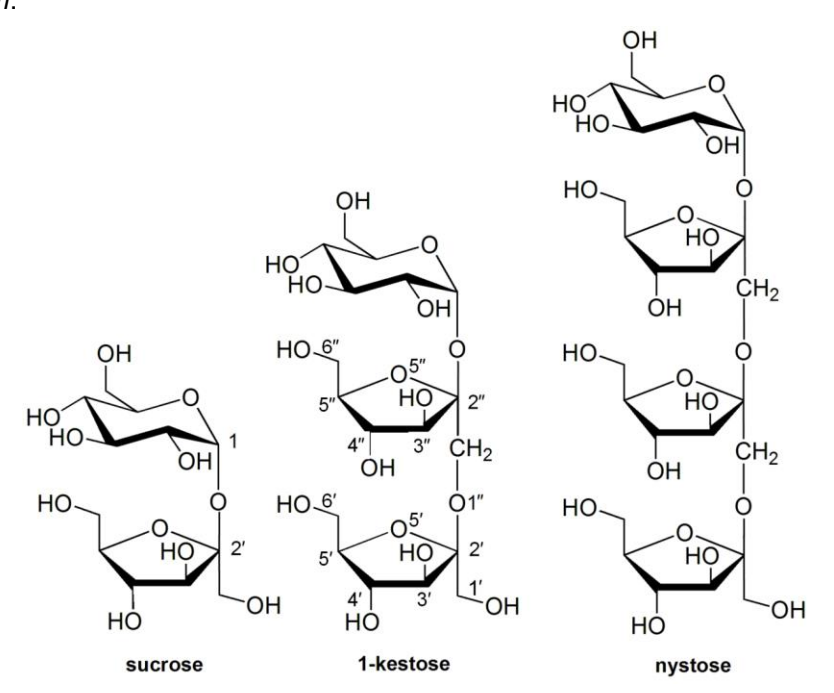


**Figure 1.** Chemical structures of sucrose, 1-kestose, and nystose, which can act as donor or acceptor substrates. Atomic labels of the furanosyl ring described in this work are also indicated.

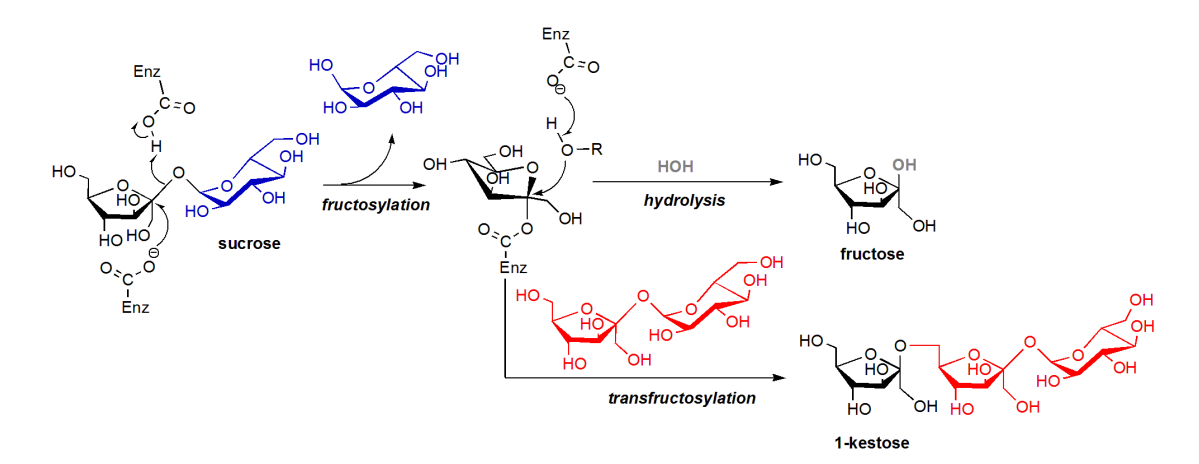
Despite the large number of microbial FT producers, only a few have demonstrated potential for industrial application and have been used in several studies about FOS production. Current research studies focus on changing operational conditions, finding novel microbial sources, or using a rational *in silico* approach to improve the efficiency in the enzymatic synthesis of FOSs <sup>3d, 4a, 5-6</sup>. Glycoside hydrolases (GHs) generally catalyze hydrolysis, but many also catalyze transglycosylation and a few GH homologues known as transglycosylases (TGs) display significant transglycosylation activities <sup>7</sup>. Since oligosaccharides can have novel nutritive and biological properties and are of use in studying enzymes used in biofuel production, producing new, efficient TG is of interest. Nowadays, there is not a straightforward, easy, and rational approach for engineering enzymes for high transglycosylation activity, mainly due to the limited knowledge of the molecular basis of transglycosylation.

The usefulness of QM/MM calculations in oligosaccharide synthesis has been demonstrated recently with the purpose to understand the mechanism of glycosides/oligosaccharide synthesis at a molecular level or (ii) to explain differences in activities between wildtype and mutant GHs  $^8$ . The first QM/MM study of the TG mechanism in GHs has been reported by Ramos's group whose research work is able to describe both hydrolysis and TG reactions of the  $\beta$ -galactosidase  $^9$ . The calculations showed that the formation of a  $\beta(1,6)$  linkage is more favorable than  $\beta(1,3)$ , thereby explaining the experimental observation. Liu and his colleague  $^8$  has successfully described the relative activities of three glycosynthase mutants (E386G, E386S and E386A) of rice BGlu1 by QM/MM calculations. They also noted that inspection of the crystal structures alone was not enough to understand the source of the different activities of the mutants. Zhang *et al.*  $^{10}$  utilized QM/MM metadynamic simulation to understand the mechanism of *Humicola insolens* Cel7B glycosynthase (E197S mutant) during flavonoid glycosides synthesis.

Here, we have investigated the detailed chemical steps of the hydrolysis and transfructosylation of a fungal fructrosyltransferase from *A. japonicas*. This enzyme belongs to the GH family GH32, which contains several other enzymes from different fungal sources (CAZy database, <sup>11</sup>). The natural acceptor substrates of fungal FT include the sucrose, 1-kestose, and nystose (Figure 1). The enzymes acts on the fructosyl donor substrate sucrose via a retaining catalytic mechanism and was shown to have high transfructosylation activity compared to other related GH32 enzymes <sup>12</sup>. However, in general, FTs are retaining enzymes that have high potential to synthesize FOS by transfructosylation. The structure of FT comprises two domains with an N-

terminal catalytic domain containing a five-blade  $\beta$ -propeller fold linked to a C-terminal  $\beta$ -sandwich domain, which contains the active site. The catalytic triad of Asp60, Asp191, and Glu292 are proposed to act as a nucleophile, transition-state stabilizer, and general acid/base catalyst, respectively. These residues contribute to the binding of the terminal fructose in the -1 subsite, in addition to the catalytic mechanism. The reaction proceeds via a double-displacement mechanism with retention of the anomeric configuration of the fructosyl moiety. Cleavage of the glycosidic bond of the donor substrate sucrose (Fru- $\beta$ -(2-1)- $\alpha$ -Glc), where Fru = fructose and Glc = glucose) has been proposed to result in the formation of a covalent enzyme- $\alpha$ -fructosyl intermediate and the release of glucose (see Scheme 1). Subsequently, the fructosyl unit can be transferred to water (see *hydrolysis*, Scheme 1) or acceptor substrates such as sucrose (see *transfructosylation*, Scheme 1), leading to the generation of fructose or 1-kestose as a final product, respectively.

Herein, we report a comparative QM/MM investigation on the sucrose hydrolysis and transfructosylation (i.e., production of 1-kestose) by *A. japonicus* FT (see Scheme 1) and demonstrate, using SCC-DFTB QM/MM calculations, why fungal FTs are capable to produce FOS from sucrose. The role of the interaction involving the donor 1-OH substrate is also explored, which supports a recent finding on *Saccharomyces cerevisiae* Gas2  $^7$ . Our study provides detailed insights into how sucrose is hydrolyzed and how FOS with  $\beta$ -(2 $\longrightarrow$ 1)-linkages is synthesized by fungal FTs. The roles of catalytic residues in the catalysis are also discussed.



**Scheme 1.** Proposed catalytic mechanism of an FT enzyme using sucrose as a donor (hydrolysis) or an acceptor (transfructosylation) to generate fructose or 1-kestose as a reaction product, respectively.

#### 2.2 Computational details

#### Model setup

The initial structure for the sucrose hydrolysis and transfructosylation steps were based on the X-ray crystal structures of the D191A mutant of A. japonicas FT in complex with sucrose and 1-kestose (solved at 2.1-2.2 Å resolution, PDB codes 3LDK and 3LDR) 12. The wildtype was recovered by manually mutating Ala191 to Asp191. For the transfructosylation, owing to the lacking of structural information for the fructosylenzyme intermediate, we thus used the X-ray crystal structure (PDB code 3LDR) of 1kestose, a transfructosylation product, as a starting point for modeling the transfructosylation reaction. All crystallographic water molecules were kept. Hydrogen atoms were added using the HBUILD subroutine in CHARMM and titratable residues in the enzyme were assigned based on the pKa estimated by PROPKA 3.1 (http://propka.ki.ku.dk) 13 at pH 7. Asp119 was assigned in a protonated form, as it is thought to enhance the nucleophilic efficiency by positioning the nucleophile Asp60 12. Glu292 were protonated, while other aspartate and glutamate residues were deprotonated. Histidine residues were assigned following the CHARMM format: HSD (protonated on ND1). HSE (protonated on NE2) or HSP (doubly protonated on ND1 and NE2). In our model system, three residues (HSP50, HSP180, HSP332) were fully protonated while other histidine residues (HSE64, HSE74, HSD79, HSE144, HSE240, HSD304) were modeled in their neutral states, with their tautomeric state assigned on the basis of the hydrogen bonding network by WHAT-IF (http://swift.cmbi.ru.nl) 14.

#### QM/MM MD simulation

To obtain the thermally equilibrated system of the two complexes, two 900-ps QM/MM MD simulations of the enzyme complex were carried out at 300 K using the same protocols applied successfully in our previous studies <sup>15</sup>. In brief, the complexes were solvated by a 25 Å radius sphere of TIP3P model waters <sup>16</sup> centered on the anomeric carbon atom (C2') of the fructosyl moeity at subsite –1 (see Figure 1). The stochastic boundary method <sup>17</sup> was used to represent environmental effects. All atoms outside the 25 Å sphere centered on C2' were deleted, while protein heavy atoms in the buffer zone (21–25 Å) were subject to Langevin dynamics with positional restraints using force constants scaled to increase from the inside to the outside of the buffer. All atoms within a 21 Å sphere of the reaction zone were subjected to Newtonian dynamics with no positional restraints. Each system was thermolized in an NVT ensemble at 300 K with a stochastic boundary QM/MM MD simulation, following the procedure described

previously <sup>15</sup>. An integration time-step of 1 fs was used, with all of the bonds involving hydrogen atoms constrained using the SHAKE algorithm <sup>18</sup>. All simulations were performed with CHARMM program <sup>19</sup>.

The QM region comprises the catalytic triad, Asp60, Asp191 and Glu292, and the substrate (sucrose/1-kestose). Hydrogen link atoms  $^{20}$  were placed between  $C_{\alpha}$  and  $C_{\beta}$  on Asp60 and Asp191 and between  $C_{\beta}$  and  $C_{\gamma}$  on Glu292. The QM regions for each reaction consist of 67 atoms (fructosylation), 46 atoms (hydrolysis), and 88 atoms (transfructosylation); all of these have a net charge of –2, corresponding to the negative charge of Asp60 and Glu292. All remaining atoms of the protein, carbohydrate, and solvent were incorporated via MM with the CHARMM force field  $^{21}$ .

## Reaction path calculations

The starting points for the QM/MM calculations were taken from several snapshots of the MD-equilibrated structures and energy minimized with QM/MM. The QM/MM calculations were carried out using the Self-Consistent-Charge Density-Functional Tight-Binding method (SCC-DFTB)  $^{22}$  as implemented in CHARMM. The SCC-DFTB method is a fast semi-empirical density functional approach that has been extensively tested and applied to several GHs  $^{15, 23}$ . The adiabatic mapping calculations were performed to explore the reaction path for the whole catalytic cycle in Scheme 1 and its reaction coordinate (r) definition will be described below. During the adiabatic mapping its value was incremented by 0.1 Å each step, using a force constant of 5000 kcal mol  $^{-1}$ Å  $^{-2}$  to drive the coordinate to each particular value. Energy minimizations at each r value were performed to within an energy gradient value of 0.01 kcal mol  $^{-1}$ Å  $^{-1}$ . The final energies were computed by a single-point calculation, removing the energy contributions due to reaction coordinate restraints.

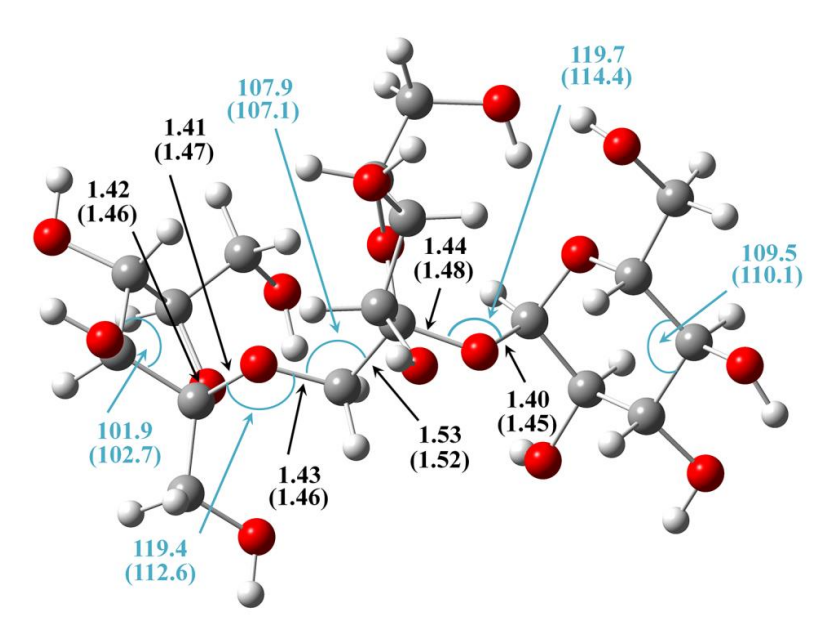


**Figure 2.** Comparison between the selected geometries of 1-kestose optimized by B3LYP/6-31++G(d,p) and SCC-DFTB (parentheses). Units for distances (black) are given in angstroms and for angles (blue), in degrees.

#### 2.3 Results and discussion

#### 2.3.1 Validation of the SCC-DFTB method

The application of the SCC-DFTB method in the elucidation of enzymatic reactivity toward carbohydrate molecules has been reported by several previous studies  $^{15,\ 23a,\ 24}.$  However, its validity remains to be checked, usually with the higher-level methods such as ab initio or DFT. It has been shown that the SCC-DFTB-optimized geometries can be compared with those obtained at the B3LYP/6-31++G(d,p) level of theorv 25. For this reason, we select 1-kestose as an example and optimized its structure in gas-phase using both the SCC-DFTB and the B3LYP/6-31++G(d,p) methods. The optimized structure of 1-kestose is displayed in Figure 2, with some selected geometric parameters labeled. Clearly, the geometries obtained by both methods are quite close, with typical bond distance difference smaller than 0.1 Å and angle difference less than 7°. Superimposition of the two optimized structures with the experimentally determined structure (PDB code 3LDR) further shows a good overlap among them, with the scissile glycosidic bond being twisted to a lesser extent in the Xray structure. We also tested its reliability in predicting reaction energetics by performing additional energy corrections at B3LYP/6-31+G(d) level on all studied reactions, employing our previous protocol <sup>15a</sup>. It is shown that both methods give qualitatively similar results. From the testing calculations above, one can see that SCC-DFTB is a valid and reasonable method for describing the structure and reactivity of the studied

enzymatic systems. Thus, the reported structures and energies discussed in the following sections are based on the QM(SCC-DFTB)/MM calculations.

# 2.3.2 Simulations of wildtype and mutant FT complex with donor/acceptor substrate

Two 900 ps QM/MM MD simulations of the sucrose—FT and 1-kestose—FT complexes in wildtype (WT) were performed to obtain the thermally equilibrated structures for modeling reactivity of FT-catalyzed hydrolysis and transfructosylation reactions. The root mean square deviations (RMSDs) for the protein heavy atoms of the simulations indicated that both complexes are quite stable and reached equilibrium after ~400 ps of simulations. Selected structural parameters of the two complexes are included in Tables 1—3. The 1-kestose—FT system exhibited a slightly higher RMSD (0.30 ± 0.01 Å) compared to the sucrose—FT system (0.21 ± 0.01 Å), owing to its longer sugar chain. Typical snapshots of the active site structures resulting from the two QM/MM MD simulations are shown in Figure 3 in comparison with the initial X-ray structures. The active site of FT consists of the side chains of Asp60 (nucleophile), Phe118, Asp119, Ile143, His144, Arg190, Ala/Asp191 (stabilizer), Glu292 (acid/base), Glu318, Ser329, His332, Tyr369, Tyr404, and Glu405 residues. These residues create an electrostatic and hydrophobic binding pocket that locked the substrate in a distorted conformation required for catalysis.

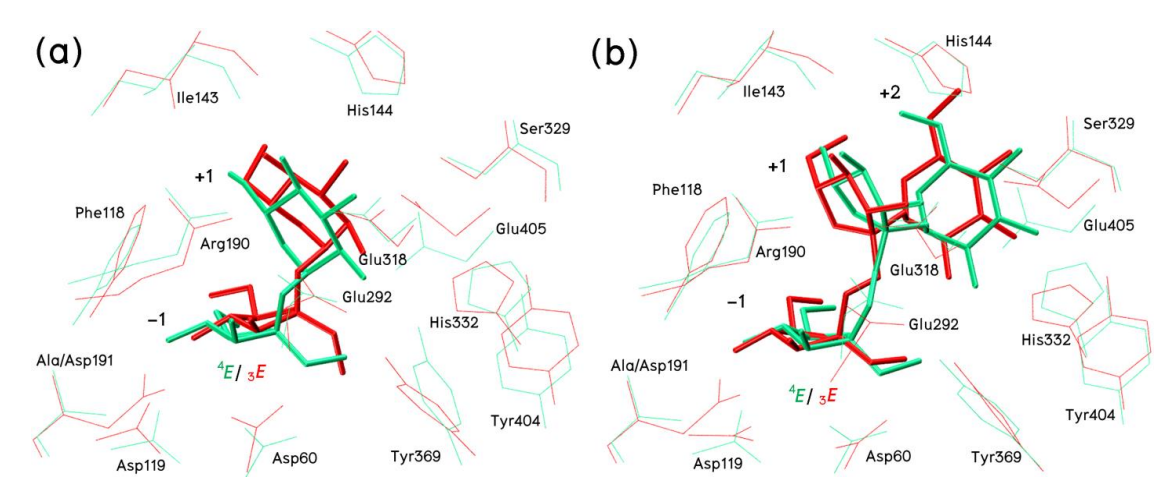


**Figure 3.** Superimposed structures of active site between the simulated (WT) and experimental (D191A) structures for the sucrose—FT (a) and 1-kestose—FT complexes (b). Structures shown in red and green color represent the equilibrated MD and X-ray structures, respectively. For clarity, substrates are shown in stick representation, while active site residues in line representation.

Table 1. Structural Parameters of Stationary Points for the First (Fructosylation) Half-Reaction Obtained from the QM(SCC-DFTB)/MM Calculations. Atom definition is indicated as Figure 5.

distances (Å), angles (°)			fructosylation		
	X-ray <sup>a</sup>	MD (RC) <sup>b</sup>	RC	TS1	IM1
$O_{\varepsilon_1}$ – $H_{\varepsilon_1}$	-	$1.01 \pm 0.03$	1.01	1.66	1.71
H <sub>ε1</sub> -O1"	_	1.81 $\pm$ 0.11	1.67	1.02	1.01
O <sub>ε1</sub> –O1"	2.83	$2.65 \pm 0.08$	2.67	2.64	2.67
C2'_O1"	1.37	$1.52 \pm 0.04$	1.53	2.38	3.26
C2'-O <sub>δ2</sub> (Asp60)	3.99	$3.66 \pm 0.30$	3.43	2.48	1.56
(Asp60)O <sub>Ō1</sub> ···HO(Asp119)	2.52 <sup>c</sup>	$1.79 \pm 0.13$	1.72	1.70	1.82
3–OH···O <sub>Ō1</sub> (Asp191)	_	$1.90 \pm 0.12$	1.82	1.72	1.73
4–OH···O <sub>δ2</sub> (Asp191)	_	$1.77 \pm 0.09$	1.74	1.69	1.72
C 5'-O5'-C2'-C3'	2.5	$15.9 \pm 7.5$	21.9	0.8	-21.3
C4'-C3'-C2'-O5'	-29.0	$-34.3 \pm 5.3$	-41.8	-23.1	-4.7

<sup>&</sup>lt;sup>a</sup> Taken from the X-ray structure of D191A-sucrose complex (PDB code 3LDK)

During the WT simulations, both substrates are quite stable and its initial conformation maintained. The superposition of the wildtype MD active-site structures of the sucrose FT and 1-kestose FT complexes with their nonproductive mutant (D191A) complexes determined experimentally displays very small RMSDs (0.49 Å and 0.25 Å, respectively) between them, indicating that the mutant has no substantial effect on the substrate binding. The mutant seems to has only minor effect on the conformation of the terminal fructose at the -1 subsite (Figure 3): it adopts a  $_3E$  conformation which is inconsistent with the nonproductive conformation ( $^4E$ ) found in the D191A mutant  $^{12}$ . Therefore, we suspect that such discrepancy in the fructose conformer derived from the MD and X-ray data may be due to the missing of hydrogen bonding interaction between the substrate and Ala191.

To test this hypothesis, we have performed another QM/MM MD simulation of the sucrose—FT complex in the D191A mutant. It is found that the mutant not only perturbed the stability of the overall system, altered the conformation of the fructosyl portion in the —1 subsite (i.e., changing from  $_3E$  in WT to  $^4E$  in D191A) but also limited the attacking position of the nucleophile (Asp60) toward the anomeric carbon C2  $^4$ 

<sup>&</sup>lt;sup>b</sup> Taken from the equilibrium QM/MM MD simulation at 600–900 ps.

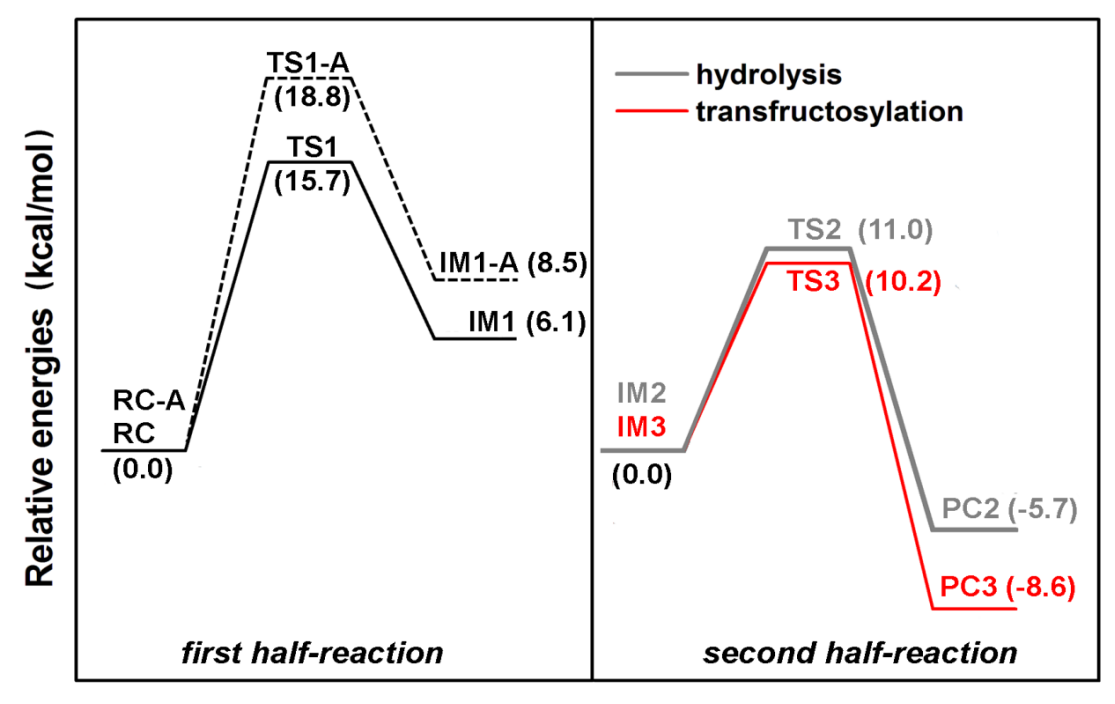
<sup>&</sup>lt;sup>c</sup> O–O distances

 $(d[C2'-O_{\bar{0}1}(D60)] = 4.11 \pm 0.19$  Å and  $d[C2'-O_{\bar{0}2}(D60)] = 3.75 \pm 0.24$  Å). This is not the case for the WT system where both distances,  $C2'-O_{\bar{0}1}(Asp60)$  and  $C2'-O_{\bar{0}2}(Asp60)$ , could be happened (Figure S3) with the average values of  $3.71 \pm 0.24$  and  $3.66 \pm 0.30$  Å, respectively, based on the QM/MM MD simulation of sucrose FT complex in the WT system.

In the equilibrated system of the sucrose complex, the carboxylate oxygen atoms ( $O_{\delta_1}$  and  $O_{\delta_2}$ ) of Asp191 forms strong, stable hydrogen bonds with two hydroxyl groups at position 3 and 4 (3 $^-$ OH and 4 $^-$ OH) of the fructosyl moiety at subsite  $^-$ 1 (3 $^-$ OH $\cdots$ O $_{\delta_1}$  = 1.90  $\pm$  0.12 Å and 4 $^-$ OH $\cdots$ O $_{\delta_2}$  = 1.77  $\pm$  0.09 Å, Table 1). The glucosyl moiety at subsite +1 is stabilized by hydrogen bonds formed by the backbone oxygen atom of Ile143 and the sidechain carboxyl group of Glu318. Glu292, an acid/base catalyst, hydrogen bonds with the glycosidic bond oxygen O1 $^{\prime\prime}$  at subsite +1 (H $_{\epsilon_1}$ -O1 $^{\prime\prime}$  = 1.81  $\pm$  0.11 Å) and is positioned 5.5 Å away from the Asp60, which supports the double displacement mechanism. Overall, Glu292 was well-positioned for proton donation to the glycosidic bond, whereas Asp60 is oriented towards the anomeric center (with a C2 $^\prime$ -O $_{\delta_2}$ (Asp60) distance of 3.66  $\pm$  0.30 Å). These interactions, as required for the first step of the sucrose hydrolysis, are maintained over the course of the simulation. For the 1-kestose system, the same interactions are also seen with additional interactions between the Tyr404 and the glucosyl moiety at subsite +2.

## 2.3.3 Reaction paths

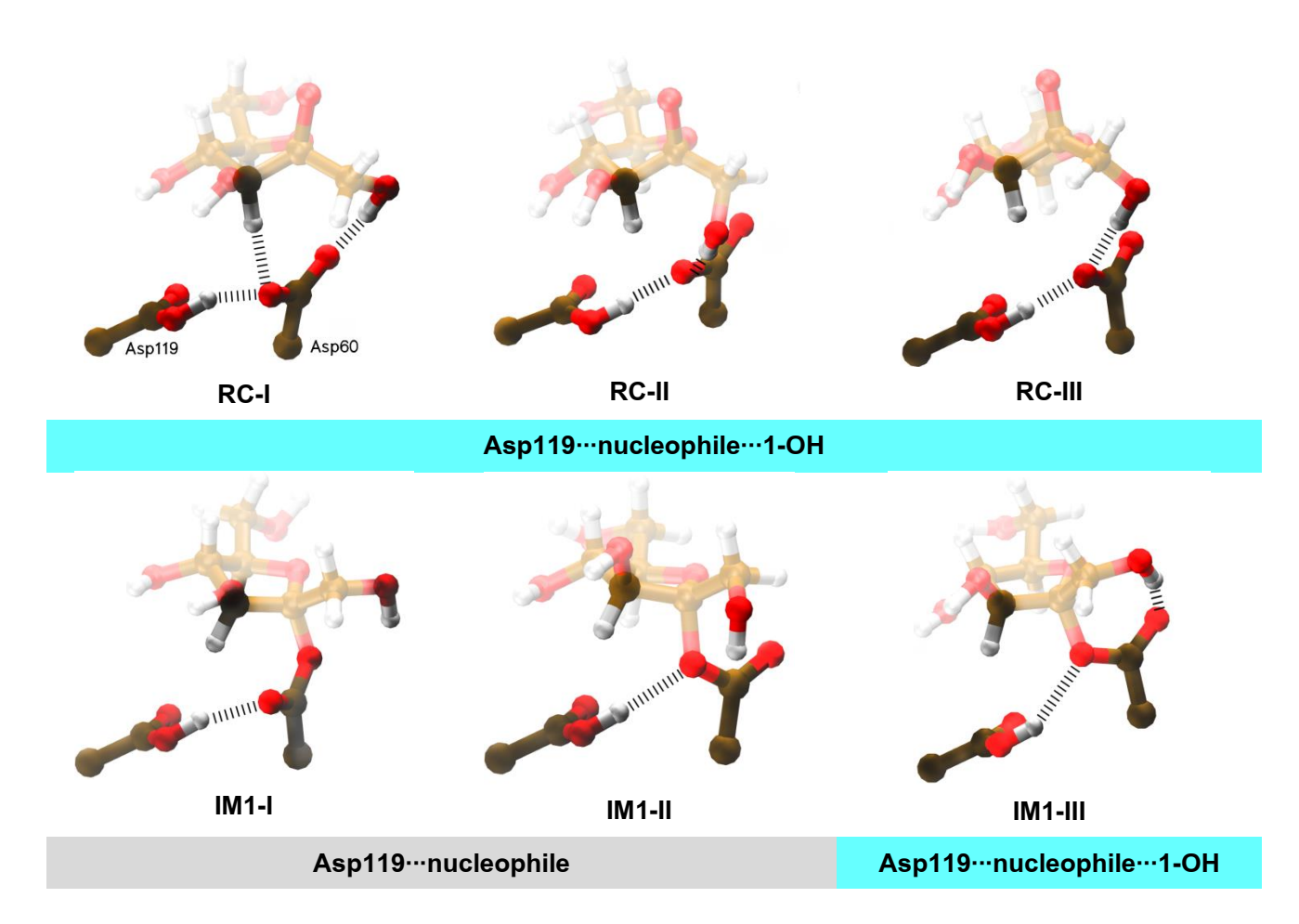
As pointed out by Chuankhayan *et al.* <sup>12</sup>, the first half-reaction (fructosylation) of the FT enzyme involves a cleavage of the glycosidic bond of the sucrose substrate and the formation of the covalent fructosyl-enzyme intermediate. Then, the glucose product must be displaced from the enzyme active site, which allows either water solvents (hydrolysis) or acceptor molecules (transfructosylation) to attack at the anomer center in the second half-reaction step. Details of the two half-reactions were discussed in the following subsections. The calculated energy profiles for the whole reaction pathways in Scheme 1 are summarized in Figure 4. All corresponding stationary points (reactant complex: **RC**, transition state: **TS**, intermediate: **IM**, and product complex: **PC**) on the profiles are illustrated in Figures 5-7.



# **Reaction coordinate**

**Figure 4.** Whole relative energy profiles for the hydrolysis and transfructosylation reactions with sucrose as donor and acceptor substrate, respectively, as shown in Scheme 1. The energy profile of the first step of the hydrolysis reaction with 1-kestose as a donor substrate is also included for comparison (shown in dash line).

Interactions involving the donor 1-OH and its impact on the energy barrier. In the work of Raich et al. <sup>7</sup>, the 2-OH group of glucose changes its hydrogen bond partner with either nucleophile or a water solvent. In our simulation, we have investigated similar interactions involved in any potential OH substituents with nucleophile and found that 1-OH seems to play a similar role, while other C3-OH and C4-OH groups of fructose participate in hydrogen bonding with Asp191. Moreover, the nucleophile Asp60 also forms hydrogen bond partner with Asp119 and/or the 1-OH as shown in Scheme 2.



**Scheme 2** Three possible interactions (Asp119···nucleophile···1-OH) involving Asp119, Asp60 (nucleophile) and 1-OH of the -1 fructose found during the formation of the fructosyl-enzyme intermediate (RC  $\rightarrow$  IM1)

To test how such different interaction in Scheme 2 affects the fructosylation energy barriers, we performed additional QM/MM calculations in the RC, TS1, and IM1 for the WT system. Regarding to this, several different active-site configurations were extracted from the QM/MM MD simulation trajectory of the sucrose-FT complex and their structures minimized. Then, we computed the minimum energy path for the formation of the fructosyl-enzyme intermediate (RC-TS1-IM1) using a linear interatomic distance,  $r_1 = [O1'', C2'] - [C2', O_{\delta_1}(Asp60)]$ , as a reaction coordinate. It is shown that the shape of the potential energy profile greatly affected by different interactions involving the Asp119, nucleophile and 1-OH (hereafter Asp119...nucleophile...1-OH). The fructosylation energy barriers for three different interactions (Scheme 2) are calculated to be 14-16 kcal mol for I, 20-21 kcal mol for II and 27 kcal mol <sup>-1</sup> for III. Notably, the reaction occurring via the Asp60-nucleophile-1-OH interaction exhibits a much higher barrier of ~10 kcal mol<sup>-1</sup>, compared to that via the Asp60-interaction. However, the T11A interaction may block the attacking of Asp60 and make the initial formation of intermediate **IM1** less likely, resulting in a drastic decrease of enzymatic activity as observed experimentally <sup>26</sup>. Thus, reaction proceeding via **I** is the most energetically preferable pathway for the first fructosylation step and the resulting stationary structures as well as selected geometries are shown in Figure 5 and Table 1.

First half-reaction: the formation of fructosyl-enzyme intermediate. To facilitate the cleavage of the  $\beta$ -(2 $\longrightarrow$ 1) linkage, Glu292 must first donate its proton H<sub>£1</sub> onto the glycosidic bond oxygen (O1"), which leads to the formation of the fructosyl-enzyme intermediate. At this stage, the proton is fully transferred to O1" to form the glucose molecule with a deprotonated Glu292 residue. During the process, the fructosyl moiety of the substrate at the -1 position changes from  ${}_{3}E$  to  ${}^{4}E$  in **TS1** and finally to  ${}_{5}E$  in **IM1**. while the glucosyl ring remains in a chair conformation  $\binom{4}{C_1}$ . The planarity of the fructosyl ring at subsite -1 at TS1 (see C5'-O5'-C2'-C3'; changing from 21.9° at RC to 0.8° at TS1) is consistent with the character of an oxocarbenium-like transition state found in many GHs active on the pyranosyl ring of carbohydrate substrate such as cellulose <sup>24</sup> and chitin <sup>15b</sup>. This step requires surmounting an energy barrier of 15.7 kcal mol and the process is endothermic by about 6 kcal mol relative to the reactant (RC). Note that no experimental rate constant  $(k_{cat})$  has been measured for hydrolytic activity of FT from A. japonicus. However,  $k_{cat}$  values for sucrose hydrolysis catalyzed by other related fructosyl-transferring enzymes from A. aculeatus, S. occidentalis, and X. dendrorhous have been reported to be between 105  $s^{-1}$  and 20460  $s^{-1}$  . corresponding to energy barriers of about 12–16 kcal mol<sup>-1</sup>. Thus, the calculated overall barrier of 15.7 kcal mol<sup>-1</sup> obtained in this study (Figure 4) is in good agreement with these observations.

We further calculated the energy profile of this step by which 1-kestose serves as a donor substrate of the reaction (i.e., the reverse of the transfructosylation) and the result is compared with the sucrose, as shown in Figure 4 (see RC-A → TS1-A → IM1-A). It is shown that the FT enzyme is more active toward sucrose than 1-kestose, giving the lower values in activation energy (15.7 vs. 18.8 kcal mol<sup>-1</sup>) and reaction energy (6.1 vs. 8.5 kcal mol<sup>-1</sup>), assuming that the first step of the reaction in both substrates is dominant. This result further supports previous biochemical studies on related enzymes which hydrolyze sucrose more efficiently than 1-kestose.

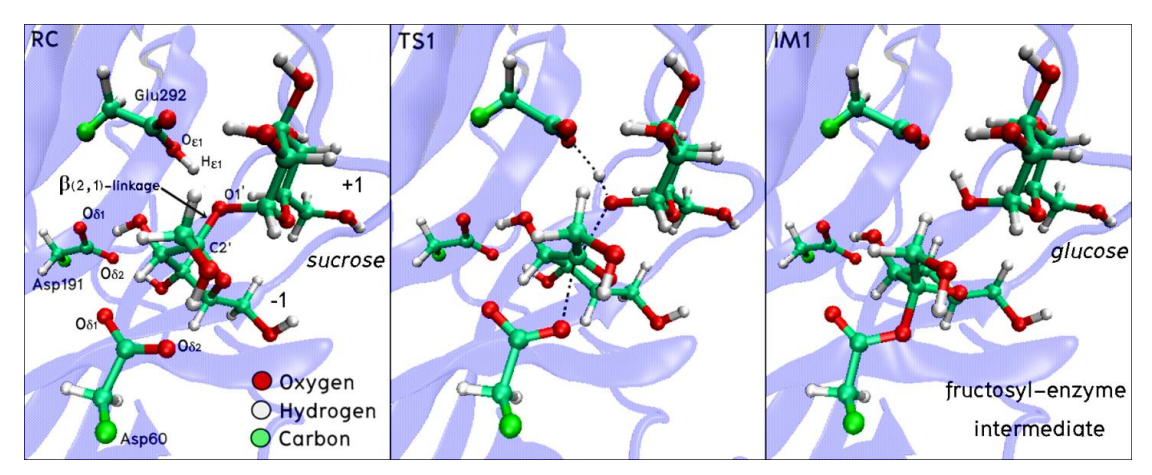


**Figure 5.** Snapshots of the stationary points for the first (fructosylation) half-reaction. For clarity, only the residues involved in the QM region are shown in the figure with ball-and-stick model. The black dashed lines represent bond breaking and forming bonds. Atom definition discussed in the text is also labeled.

Second half-reaction: hydrolysis of the fructosyl-enzyme intermediate. After the departure of the glucose product, a water molecule competes with a nearby acceptor molecule to come into the active site and acts as the nucleophile in the second halfreaction with Glu292 serving as the general base to activate this water molecule. To model this reaction step, we first removed the product from the active site and allowed some water molecules to fill the cavity. The position of the attacking water was manually placed in proximity to the C2 atom. These water molecules were minimized and the entire protein system was further relaxed by another MD simulation. Several snapshots from the equilibrium state (600-900 ps) were used for the reaction path calculations. Starting from a snapshot extracted from the simulation, we calculated the energy profile for the hydrolysis process (IM2 $\rightarrow$ TS2 $\rightarrow$ PC2) using a reaction coordinate defined as  $r_2$ =  $[C2' - O_{\delta_1}(Asp60)] - [C2' - O_w]$  (see also Figure S2). The stationary structures are visualized in Figure 6 and the selected structural parameters are tabulated in Table 2. Like the process of fructosylation, the carboxylate group of the Glu292 accepts a proton from the water nucleophile. The transition state TS2 was found to have transient bonds  $C2'-O_w$  and  $C2'-O_{\delta_1}(Asp60)$  of 2.32 and 2.22 Å, respectively (Table 2). The conformation at the anomeric center C2 changes from  $_5E$  in IM2 to  $^4E$  in TS2 to facilitate the attacking of nucleophile, which then end up for this hydrolysis process with <sub>3</sub>E. Such a distortion of the furanose ring at subsite -1 is once again confirmed by the change of the C5-O5-C2-C3 dihedral angle as shown in Table 2. With the

elongation of the  $C2'-O_{\delta_1}(Asp60)$  bond from 1.56 to 3.47 Å, the covalent fructosylenzyme bond is finally broken, and the Glu292 is also protonated again to complete the catalytic cycle of sucrose hydrolysis. This step requires an energy barrier of about 11 kcal mol<sup>-1</sup> (Figure 4) in order to generate a fructose molecule as product (see **PC2**, Figure 6). It is found that the barrier of the hydrolysis process is significantly lower than that of the first half-reaction (15.7 kcal mol<sup>-1</sup>), as shown in Figure 4.

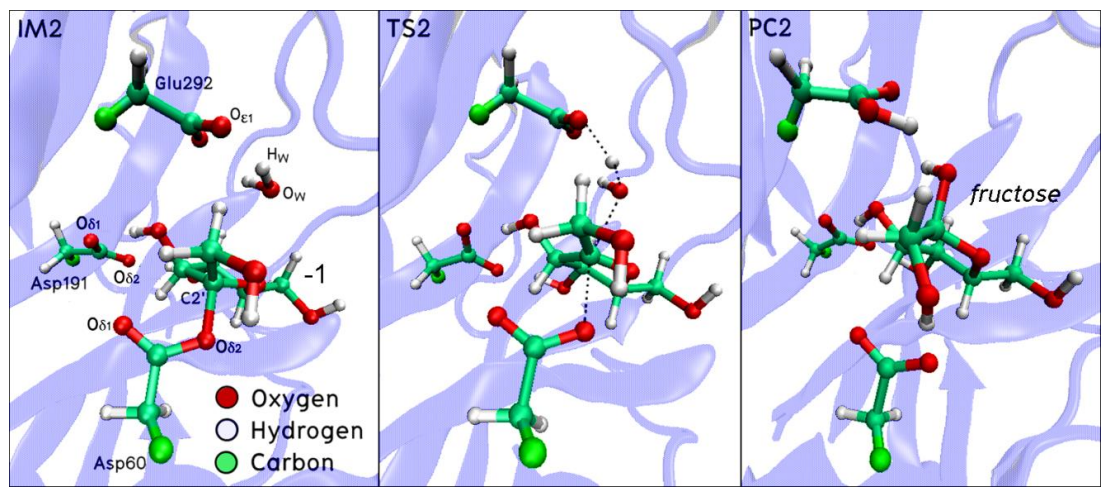


**Figure 6.** Snapshots of the stationary points for the second (hydrolysis) half-reaction. For clarity, only the residues involved in the QM region are shown in the figure with ball-and-stick model. The black dashed lines represent bond breaking and forming bonds. Atom definition discussed in the text is also labeled.

Table 2. Structural Parameters of Stationary Points for the Second (Hydrolysis) Half-Reaction Obtained from the QM(SCC-DFTB)/MM Calculations. Atom definition is indicated as Figure 6.

		hydrolysis		
distances (Å), angles (°)	MD(IM2) <sup>a</sup>	IM2	TS2	PC2
O <sub>E1</sub> –H <sub>w</sub>	$2.48 \pm 0.64$	1.71	1.55	1.02
$H_w$ – $O_w$	$0.98 \pm 0.02$	1.01	1.04	1.72
C2 <b>'</b> -O <sub>w</sub>	$3.49 \pm 0.13$	3.56	2.32	1.47
C2 <b>′</b> -O <sub>δ2</sub> (Asp60)	$1.53 \pm 0.04$	1.56	2.22	3.47
(Asp60)O <sub>Ō1</sub> ···HO(Asp119)	$2.00\pm0.25$	1.85	1.71	1.70
3–OH···O <sub>Ō1</sub> (Asp191)	$1.96 \pm 0.22$	1.68	1.72	1.82
4–OH···O <sub>δ2</sub> (Asp191)	$1.77 \pm 0.12$	1.75	1.73	1.75
C5'-O5'-C2'-C3'	$-20.4 \pm 7.8$	26.1	-7.8	9.1
C4'-C3'-C2'-O5'	1.9 $\pm$ 9.5	-1.9	-14.7	-32.0

<sup>&</sup>lt;sup>a</sup> Taken from the equilibrium QM/MM MD simulation at 600–900 ps

Second half-reaction: transfructosylation. As mentioned previously, the initial structure for modeling this reaction step (IM3 -> TS3 -> PC3) was taken from a crystal structure of FT bound with 1-kestose (PDB code 3LDR), a product of the transfructosylation, which was then subjected to a QM/MM MD simulation for 1200 ps. To model this step, we performed both reverse and forward reactions using different MD snapshots, as starting points (PC3), along with  $r_3 = [C2',O1''] - [C2',O_{\bar{0}1}(Asp60)]$ . The energy profile is shown in Figure 4. The resulting optimized structures are shown in Figure 8 and their selected geometries are tabulated in Table 3. The sucrose acceptor is hydrogen bonded, via its 1-OH group, with a carboxylate group of Glu292 with an  $O_{E1}$ - $H_{E1}$  distance of 1.70 Å and is 3.32 Å away from the anomer atom C2 (see IM3, Figure 7). Break down of the intermediate (IM3) occurs concomitantly with the formation of the glycosidic bond, as can be seen by the shortening of the C2'-O1" bond (3.32 Å at IM3  $\rightarrow$  2.25 Å at TS3 Å  $\rightarrow$  1.52 Å at PC3) and elongation of the C2  $^{\prime}$ -O $_{\bar{0}_1}$ (Asp60) bond (1.53 Å at IM3  $\rightarrow$  2.35 Å at TS3 Å  $\rightarrow$  3.22 Å at PC3). At the same time, Glu292 abstracts a proton (H<sub>E1</sub>) from the hydroxyl group of the sucrose acceptor. The shortening of the 3-OH···O $\delta_2$ (Asp191) distance from 1.78 Å at IM3 to 1.72 Å at PC3 clearly indicates the role of Asp191 in substrate distortion. Near planarity (C5′-O5′-C2′-C3' = 2.8 Å) is also found at **TS3**, as has been found in **TS1**. In this step, the proton transfer takes place before the breakdown of the intermediate. This process requires 10.2 kcal mol<sup>-1</sup> and is exothermic by about 9 kcal mol<sup>-1</sup> relative to **IM3** (see Figure 4). The 1-kestose product (PC3) appears to be more stable than the hydrolysis product (PC2), which is expected from its additional hydrogen bonds with residues at subsites +1 and +2. In an opposite manner to the first half-reaction, the conformation of the -1 Fruc unit changes from  ${}_{5}E$  in **IM3** to  ${}^{4}E$  in **TS3** and finally to  ${}_{3}E$  in **PC3**, while other Fruc and Glc units at the positive subsite maintained its envelope and chair conformation, respectively.

It is interestingly to noted here that the barrier for both hydrolysis and transfructosylation is quite similar (10.2 vs. 11.0 kcal mol<sup>-1</sup>), which further suggests that the two processes would compete with each other if the water and the acceptor sucrose have the same concentration in the productive position. This result also supports a previous report of Ghazi *et al.* <sup>6b</sup> on the kinetics of the hydrolytic and transfructosylation reactions of *A. aculeatus* FT. Using transition state theory, the reported kinetic parameters of the two reactions correspond to the energy barriers of about 15 kcal

mol<sup>-1</sup> (hydrolysis) and 13 kcal mol<sup>-1</sup> (transfructosylation), showing the same trend as found in our QM/MM calculations.

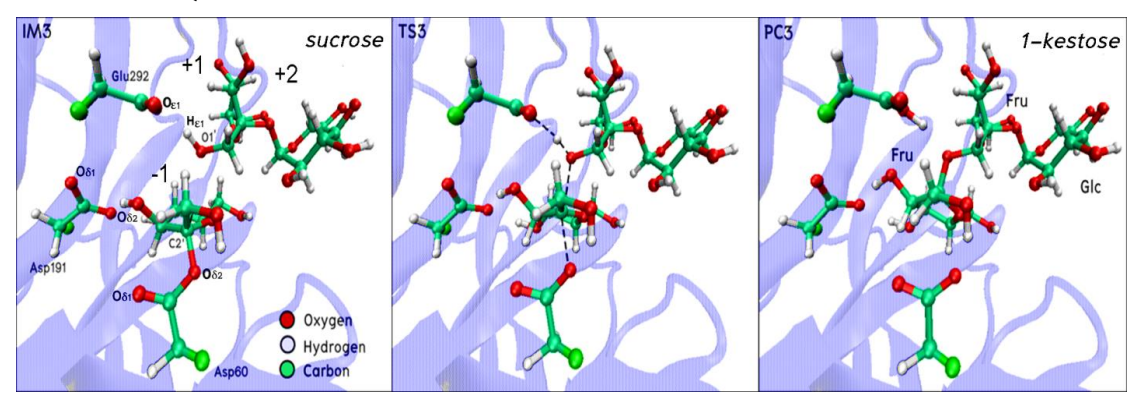


**Figure 7.** Snapshots of the stationary points for the second (transfructosylation) half-reaction. For clarity, only the residues involved in the QM region are shown in the figure with ball-and-stick model. The black dashed lines represent bond breaking and forming bonds. Atom definition discussed in the text is also labeled.

Table 3. Structural Parameters of Stationary Points for the Second (Transfructosylation) Half-Reaction Obtained from the QM(SCC-DFTB)/MM Calculations. Atom Definition is Indicated as Figure 7.

distances (Å), angles (°)	transfructosylation				
	IM3	TS3	PC3	MD(PC3) <sup>a</sup>	X-ray <sup>b</sup>
$O_{\varepsilon_1}$ – $H_{\varepsilon_1}$	1.70	1.60	1.02	1.01 ± 0.03	_
H <sub>ε1</sub> -O1"	1.01	1.03	1.68	1.72 $\pm$ 0.11	2.84 <sup>c</sup>
C2'-O1"	3.32	2.25	1.52	$1.52 \pm 0.04$	1.48
C2'-O <sub>δ2</sub> (Asp60)	1.52	2.35	3.22	$3.40 \pm 0.19$	3.09
$(Asp60)O_{\bar{0}1}$ ···HO $(Asp119)$	1.89	1.71	1.70	$1.78 \pm 0.10$	2.65°
3 <sup>-</sup> OH···O <sub>δ2</sub> (Asp191)	1.78	1.76	1.72	1.85 $\pm$ 0.26	_
4 <sup>-</sup> OH···O <sub>δ2</sub> (Asp191)	1.75	1.73	1.77	$1.80 \pm 0.11$	_
C4'-C5'-O5'-C2'	34.5	16.2	1.0	$1.3 \pm 6.1$	2.2
C5'-O5'-C2'-C3'	-17.8	2.8	21.8	$22.6 \pm 6.0$	25.0
C4'-C3'-C2'-O5'	<b>-</b> 5.7	-20.5	-35.5	$-37.5 \pm 4.8$	-26.7

<sup>&</sup>lt;sup>a</sup> Taken from the equilibrium QM/MM MD simulation at 600–900 ps.

# 2.3.4 Residue contributions to electrostatic stabilization

Analysis of the interaction of the reacting system with the protein environment can identify key groups involved in stabilizing transition states and intermediates in

<sup>&</sup>lt;sup>b</sup> Taken from the X-ray structure of D191A-FT complex with 1-kestose (PDB code 3LDR)

<sup>&</sup>lt;sup>c</sup> O–O distances

enzymes  $^{15a, 29}$ . The interaction energies of protein residues in the environment (treated by molecular mechanics, MM) with the reacting system (treated quantum mechanically, QM) are calculated for the key step of the reaction (here **RC**, **TS1**, and **IM1**). For each complex, the QM/MM interaction energy with and without each selected residue deleted was evaluated  $^{15a}$ . Positive and negative values of  $\Delta E(\text{QM/MM}_{\text{elec}})$  indicate that the residue stabilizes or destabilizes the reacting system, respectively. This method was used to identify the effect of active site residues on the energy barrier of the rate-determining (fructosylation) step of the reaction catalyzed by the FT enzyme (Figure 3). Results are presented in Table 4. It is found that Glu318 has a destabilizing effect on the **TS1** and **IM1** of -7.3 and -12.1 kcal mol $^{-1}$ . Arg190 interacts through hydrogen bonds with sucrose and have a strongest stabilizing effect on both **TS1** and **IM1** of 12.9 and 13.2, respectively. Residue Asp119 interacts through hydrogen bonds with the nucleophile Asp60, slightly stabilizing and destabilizing the **TS1** and **IM1**, respectively.

Table 4 Changes of the  $\Delta E(QM/MM_{elec})$  Stabilization Energies ( $\Delta\Delta E$  in kcal mol<sup>-1</sup>) Due to the Electrostatic Contribution of the Key Residues in Table S1

Residue deleted	Δ	ΔE
	$RC \rightarrow TS1$	RC  o IM1
Asp119	1.3	<b>-</b> 1.4
Arg190	12.9	13.2
Glu318	<b>-</b> 7.3	<b>-</b> 12.1
His332	5.2	7.9

#### 2.4 Conclusion

In this study, the QM/MM calculations were performed to understand the catalytic mechanism and energetic origin for the preference of the FOS production by a fungal FT. In particular, we examined the transition state structures and energetics of both hydrolysis and transfructosylation reactions of the enzyme. For the fructosylation process, the cleavage of the  $\beta$ -(2 $\longrightarrow$ 1) linkage of the sucrose substrate follows an S<sub>N</sub>2-like mechanism, in which the protonation of glycoside oxygen taking place prior to the breaking of glycosidic bond. The formation of fructosyl-enzyme intermediate was calculated to be the rate-determining step of the whole catalytic process, with the energy barrier of 15.7 kcal mol  $^{-1}$ , in good agreement with the reported experimental data. Our calculations indicate similar values of the deglycosylation barriers (~10 kcal

mol $^{-1}$ ) in both steps (hydrolysis and transfructosylation), which could explain from the energetically point of view why this fungal enzyme is capable to synthesize the FOS. For each reaction step, a conformational change ( $_3E \leftrightarrow ^4E \leftrightarrow _5E$ ) is observed in the fructosyl ring at subsite -1 with the transition state featuring an oxocarbonium. Moreover, our results also support the higher hydrolytic activity of sucrose over 1-kestose, by showing that FT has an energetic preference for the hydrolysis of sucrose rather than that of 1-kestose. The importance of residues Arg190 and His332 in stabilizing the **TS1** and **IM1** during the key (fructosylation) step of the overall reaction are also highlighted. The detailed information obtained in this study contributes to a better understanding on the FOS synthesis process, which can be applied to other FOS-synthesizing enzyme FT and may help further protein engineering research.

#### References

- 1. (a) Fanaro, S.; Boehm, G.; Garssen, J.; Knol, J.; Mosca, F.; Stahl, B.; Vigi, V., Galacto-oligosaccharides and long-chain fructo-oligosaccharides as prebiotics in infant formulas: A review. *Acta Pediatr.* **2005**, *94*, 22-26; (b) Knol, J.; Scholtens, P.; Kafka, C.; Steenbakkers, J.; Gro, S.; Helm, K.; Klarczyk, M.; Schopfer, H.; Bockler, H. M.; Wells, J., Colon microflora in infants fed formula with galacto- and fructo-oligosaccharides: more like breast-fed infants. *J. Pediatr. Gastroenterol. Nutr.* **2005**, *40* (1), 36-42.
- 2. Belorkar, S. A.; Gupta, A. K., Oligosaccharides: a boon from nature's desk. *AMB Express* **2016**, *6* (1), 82.
- (a) Baciu, I. E.; Jordening, H. J.; Seibel, J.; Buchholz, K., Investigations of the transfructosylation reaction by fructosyltransferase from B. subtilis NCIMB 11871 for the synthesis of the sucrose analogue galactosyl-fructoside. J. Biotechnol. 2005, 116 (4), 347-57; Paulino, R. J. V.; Zuniga-Hansen, M. E., Sucrose transfructosylation to fructooligosaccharides by the application of commercial enzymes. J. Biotechnol. 2010, 150, Supplement, 334; (c) Vega-Paulino, R. J.; Zúniga-Hansen, M. E., Potential application of for commercial enzyme preparations industrial production of short-chain fructooligosaccharides. J. Mol. Catal. B-Enzym. 2012, 76, 44-51; (d) Zambelli, P.; Fernandez-Arrojo, L.; Romano, D.; Santos-Moriano, P.; Gimeno-Perez, M.; Poveda, A.; Gandolfi, R.; Fernández-Lobato, M.; Molinari, F.; Plou, F. J., Production of fructooligosaccharides by mycelium-bound transfructosylation activity present in Cladosporium cladosporioides and Penicilium sizovae. Process Biochemi. 2014, 49 (12), 2174-2180.
- 4. (a) Maiorano, A. E.; Piccoli, R. M.; da Silva, E. S.; de Andrade Rodrigues, M. F., Microbial production of fructosyltransferases for synthesis of pre-biotics. *Biotechnol. Lett.* **2008**, *30* (11), 1867-77; (b) Sangeetha, P. T.; Ramesh, M. N.; Prapulla, S. G., Recent trends in the

- microbial production, analysis and application of fructooligosaccharides. *Trends Food Sci. Technol.* **2005**, *16*; (c) Yun, J. W., Fructooligosaccharides—occurrence, preparation, and application. *Enzyme Microb. Technol.* **1996**, *19* (2), 107-117.
- 5. Huang, M.-P.; Wu, M.; Xu, Q.-S.; Mo, D.-J.; Feng, J.-X., Highly efficient synthesis of fructooligosaccharides by extracellular fructooligosaccharide-producing enzymes and immobilized cells of Aspergillus aculeatus M105, and purification and biochemical characterization of a fructosyltransferase from the fungus. *J. Agric. Food Chem.* **2016**, *64* (33), 6425-6432.
- (a) Ganaje, A.; Lateef, A.; Gupta, U. S., Enzymatic fructooligosaccharides production by microorganisms. Appl Biotechnol 2014, 172; (b) Ghazi, I.; Fernandez-Arrojo, L.; Garcia-Arellano, H.; Ferrer, M.; Ballesteros, A.; Plou, F. J., Purification and kinetic characterization of a fructosyltransferase from Aspergillus aculeatus. J. Biotechnol. 2007, 128 (1), 204-211; (c) Zhang, L.; An, J.; Li, L.; Wang, H.; Liu, D.; Li, N.; Cheng, H.; Deng. Z., Highly efficient fructooligosaccharides production by an erythritol producing yeast Yarrowia lipolytica displaying fructosyltransferase. J. Agric. Food Chem. 2016, 64 (19), 3828-3837; (d) Alméciga-Díaz, C. J.; Gutierrez, Á. M.; Bahamon, I.; Rodríguez, A.; Rodríguez, M. A.; Sánchez, O. F., Computational analysis of the fructosyltransferase enzymes in plants, fungi and bacteria. Gene 2011, 484 (1-2), 26-34; (e) Olarte-Avellaneda, S.; Rodríguez-López, A.; Patiño, J. D.; Alméciga-Díaz, C. J.; Sánchez, O. F., In silico analysis of the structure of fungal fructooligosaccharides-synthesizing enzymes. Interdiscip. Sci. 2016, 1-15; (f) Rodríguez, M. A.; Sánchez, O. F.; Alméciga-Díaz, C. J., Gene cloning and enzyme structure modeling of the Aspergillus oryzae N74 fructosyltransferase. Mol. Biol. Rep. 2011, 38 (2), 1151-1161.
- 7. Raich, L.; Borodkin, V.; Fang, W.; Castro-López, J.; van Aalten, D. M. F.; Hurtado-Guerrero, R.; Rovira, C., A trapped covalent intermediate of a glycoside hydrolase on the pathway to transglycosylation. Insights from experiments and quantum mechanics/molecular mechanics simulations. *J. Am. Chem. Soc* **2016**, *138* (10), 3325-3332.
- 8. Wang, J.; Pengthaisong, S.; Cairns, J. R. K.; Liu, Y., X-ray crystallography and QM/MM investigation on the oligosaccharide synthesis mechanism of rice BGlu1 glycosynthases. *Biochimica et Biophysica Acta (BBA) Proteins and Proteomics* **2013**, *1834* (2), 536-545.
- 9. Bras, N. F.; Fernandes, P. A.; Ramos, M. J., QM/MM Studies on the beta-Galactosidase Catalytic Mechanism: Hydrolysis and Transglycosylation Reactions. *Journal of chemical theory and computation* **2010**, 6 (2), 421-33.
- 10. Zhang, Y.; Yan, S.; Yao, L., Mechanism of the Humicola insolens Cel7B E197S mutant catalyzed flavonoid glycosides synthesis: a QM/MM metadynamics simulation study. *Theor. Chem. Acc.* **2013**, *132* (6), 1367.

- 11. Lombard, V.; Golaconda Ramulu, H.; Drula, E.; Coutinho, P. M.; Henrissat, B., The carbohydrate-active enzymes database (CAZy) in 2013. *Nucleic Acids Res.* **2014**, *42* (Database issue), D490-D495.
- 12. Chuankhayan, P.; Hsieh, C.-Y.; Huang, Y.-C.; Hsieh, Y.-Y.; Guan, H.-H.; Hsieh, Y.-C.; Tien, Y.-C.; Chen, C.-D.; Chiang, C.-M.; Chen, C.-J., Crystal structures of Aspergillus japonicus fructosyltransferase complex with donor/acceptor substrates reveal complete subsites in the active site for catalysis. *J. Biol. Chem.* **2010**, *285* (30), 23251-23264.
- 13. Olsson, M. H.; Sondergaard, C. R.; Rostkowski, M.; Jensen, J. H., PROPKA3: consistent treatment of internal and surface residues in empirical pKa predictions. *J. Chem. Theory Comput.* **2011**, *7* (2), 525-37.
- 14. Vriend, G., WHAT IF: A molecular modeling and drug design program. *J. Mol. Graph.* **1990**, *8* (1), 52-56.
- 15. (a) Jitonnom, J.; Lee, V. S.; Nimmanpipug, P.; Rowlands, H. A.; Mulholland, A. J., Quantum mechanics/molecular mechanics modeling of substrate-assisted catalysis in family 18 chitinases: conformational changes and the role of Asp142 in catalysis in ChiB. *Biochemistry* **2011**, *50* (21), 4697-711; (b) Jitonnom, J.; Limb, M. A.; Mulholland, A. J., QM/MM free-energy simulations of reaction in Serratia marcescens Chitinase B reveal the protonation state of Asp142 and the critical role of Tyr214. *J. Phys. Chem. B* **2014**, *118* (18), 4771-83.
- 16. Jorgensen, W. L.; Chandrasekhar, J.; Madura, J. D.; Impey, R. W.; Klein, M. L., Comparison of simple potential functions for simulating liquid water. *J. Chem. Phys.* **1983**, 79 (2), 926.
- 17. Brooks, B. R.; Bruccoleri, R. E.; Olafson, B. D.; States, D. J.; Swaminathan, S.; Karplus, M., CHARMM: A program for macromolecular energy, minimization, and dynamics calculations. *J. Comput. Chem.* **1983**, *4* (2), 187-217.
- 18. Ryckaert, J.-P.; Ciccotti, G.; Berendsen, H. J. C., Numerical integration of the cartesian equations of motion of a system with constraints: molecular dynamics of n-alkanes. *J. Comp. Phys.* **1977**, *23* (3), 327-341.
- 19. Brooks, C. L.; Karplus, M., Deformable stochastic boundaries in molecular dynamics. *J. Chem. Phys* **1983**, 79 (12), 6312.
- 20. Singh, U. C.; Kollman, P. A., A combined ab initio quantum mechanical and molecular mechanical method for carrying out simulations on complex molecular systems: Applications to the CH3Cl + Cl— exchange reaction and gas phase protonation of polyethers. *J. Comp. Chem.* **1986,** 7 (6), 718-730.
- 21. MacKerell, A. D.; Bashford, D.; Bellott, M.; Dunbrack, R. L.; Evanseck, J. D.; Field, M. J.; Fischer, S.; Gao, J.; Guo, H.; Ha, S.; Joseph-McCarthy, D.; Kuchnir, L.; Kuczera, K.; Lau, F. T. K.; Mattos, C.; Michnick, S.; Ngo, T.; Nguyen, D. T.; Prodhom, B.; Reiher, W. E.; Roux,

- B.; Schlenkrich, M.; Smith, J. C.; Stote, R.; Straub, J.; Watanabe, M.; Wiórkiewicz-Kuczera, J.; Yin, D.; Karplus, M., All-atom empirical potential for molecular modeling and dynamics studies of proteins. *J. Phys. Chem. B* **1998**, *102* (18), 3586-3616.
- 22. Cui, Q.; Elstner, M.; Kaxiras, E.; Frauenheim, T.; Karplus, M., A QM/MM implementation of the self-consistent charge density functional tight binding (SCC-DFTB) method. *J. Phys. Chem. B* **2001**, *105* (2), 569-585.
- 23. (a) Islam, S. M.; Roy, P.-N., Performance of the SCC-DFTB model for description of five-membered ring carbohydrate conformations: comparison to force fields, highlevel electronic structure methods, and experiment. *J. Chem. Theory Comput.* **2012**, *8* (7), 2412-2423; (b) Barnett, C. B.; Naidoo, K. J., Ring puckering: a metric for evaluating the accuracy of AM1, PM3, PM3CARB-1, and SCC-DFTB carbohydrate QM/MM simulations. *J. Phys. Chem. B* **2010**, *114* (51), 17142-17154.
- 24. Liu, J.; Wang, X.; Xu, D., QM/MM study on the catalytic mechanism of cellulose hydrolysis catalyzed by cellulase Cel5A from Acidothermus cellulolyticus. *The journal of physical chemistry. B* **2010**, *114* (3), 1462-70.
- 25. Elstner, M.; Cui, Q.; Munih, P.; Kaxiras, E.; Frauenheim, T.; Karplus, M., Modeling zinc in biomolecules with the self consistent charge-density functional tight binding (SCC-DFTB) method: Applications to structural and energetic analysis. *J. Comp. Chem.* **2003**, *24* (5), 565-581.
- 26. (a) Homann, A.; Biedendieck, R.; Götze, S.; Jahn, D.; Seibel, J., Insights into polymer versus oligosaccharide synthesis: mutagenesis and mechanistic studies of a novel levansucrase from Bacillus megaterium. *Biochem. J.* **2007**, *407* (Pt 2), 189-198; (b) Ortiz-Soto, M. E.; Rivera, M.; Rudino-Pinera, E.; Olvera, C.; Lopez-Munguia, A., Selected mutations in Bacillus subtilis levansucrase semi-conserved regions affecting its biochemical properties. *Protein Eng. Des. Sel.* **2008**, *21* (10), 589-95.
- 27. (a) Linde, D.; Macias, I.; Fernández-Arrojo, L.; Plou, F. J.; Jiménez, A.; Fernández-Lobato, M., Molecular and biochemical characterization of a β-Fructofuranosidase from Xanthophyllomyces dendrorhous. *Appl. Environ. Microbiol.* **2009**, *75* (4), 1065-1073; (b) Alvaro-Benito, M.; Sainz-Polo, M. A.; Gonzalez-Perez, D.; Gonzalez, B.; Plou, F. J.; Fernandez-Lobato, M.; Sanz-Aparicio, J., Structural and kinetic insights reveal that the amino acid pair Gln-228/Asn-254 modulates the transfructosylating specificity of Schwanniomyces occidentalis beta-fructofuranosidase, an enzyme that produces prebiotics. *J. Biol. Chem.* **2012**, *287* (23), 19674-86; (c) Ramirez-Escudero, M.; Gimeno-Perez, M.; Gonzalez, B.; Linde, D.; Merdzo, Z.; Fernandez-Lobato, M.; Sanz-Aparicio, J., Structural analysis of beta-fructofuranosidase from Xanthophyllomyces dendrorhous reveals unique features and the crucial role of N-glycosylation in oligomerization and activity. *J. Biol. Chem.* **2016**; (d) Álvaro-Benito, M.; de Abreu, M.; Portillo, F.; Sanz-Aparicio, J.; Fernández-Lobato, M., New insights

into the fructosyltransferase activity of Schwanniomyces occidentalis ß-fructofuranosidase, emerging from nonconventional codon usage and directed mutation. *Appl. Environ. Microbiol.* **2010,** 76 (22), 7491-7499.

- 28. Gutiérrez-Alonso, P.; Fernández-Arrojo, L.; Plou, F. J.; Fernández-Lobato, M., Biochemical characterization of a  $\beta$ -fructofuranosidase from Rhodotorula dairenensis with transfructosylating activity. *FEMS Yeast Res.* **2009**, 9 (5), 768-773.
- 29. (a) Ranaghan, K. E.; Ridder, L.; Szefczyk, B.; Sokalski, W. A.; Hermann, J. C.; Mulholland, A. J., Transition state stabilization and substrate strain in enzyme catalysis: ab initio QM/MM modelling of the chorismate mutase reaction. *Org. Biomol. Chem.* **2004**, *2* (7), 968-980; (b) Ranaghan, K. E.; Ridder, L.; Szefczyk, B.; Sokalski, W. A.; Hermann, J. C.; Mulholland, A. J., Insights into enzyme catalysis from QM/MM modelling: transition state stabilization in chorismate mutase. *Mol. Phys.* **2003**, *101* (17), 2695-2714; (c) Hermann, J. C.; Ridder, L.; Holtje, H. D.; Mulholland, A. J., Molecular mechanisms of antibiotic resistance: QM/MM modelling of deacylation in a class A β-lactamase. *Org. Biomol. Chem.* **2006**, *4* (2), 206-10; (d) Hermann, J. C.; Hensen, C.; Ridder, L.; Mulholland, A. J.; Holtje, H. D., Mechanisms of antibiotic resistance: QM/MM modeling of the acylation reaction of a class A β-lactamase with benzylpenicillin. *J. Am. Chem. Soc.* **2005**, *127* (12), 4454-65.

- 1. ผลงานตีพิมพ์ในวารสารวิชาการนานาชาติ (ระบุชื่อผู้แต่ง ชื่อเรื่อง ชื่อวารสาร ปี เล่มที่ เลขที่ และหน้า) หรือผลงานตามที่คาดไว้ในสัญญาโครงการ
  - 1.1 บทความวิจัยระดับนานาชาติที่ได้รับการตีพิมพ์ (และ/หรือกำลังอยู่ใน ขั้นตอน) ในฐานข้อมูล SCOPUS/ISI และมีค่า impact factor จำนวน ทั้งสิ้น 4 เรื่อง

# ก. บทความหลักที่คาดไว้ในสัญญาโครงการ จำนวน 1 เรื่อง

**Jitonnom J.**, Ketudat Cairns JR, Hannongbua S, QM/MM modeling of the hydrolysis and transfructosylation reactions of fructosyltransferase from Aspergillus japonicas, an enzyme that produces prebiotic fructooligosaccharide, *submitted*.

# ข. บทความอื่นๆ ที่ต่อยอดจากงานวิจัยหลักของโครงการ จำนวน 3 เรื่อง

**Jitonnom J.**, Meelua W. Effect of ligand structure in the trimethylene carbonate polymerization by cationic zirconocene catalysts: A "naked model" DFT study. J. Organometal. Chem., 2017, 841, 48-56. (IF: 2.336)

**Jitonnom J.**, Meelua W. Cationic ring-opening polymerization of cyclic carbonates and lactones by group 4 metallocenes: A theoretical study on mechanism and ring-strain effects. J. Theor. Comput. Chem., 2017, 16, 1750003 (IF: 0.619)

**Jitonnom J.**, Molloy R., Punyodom W., Meelua W. Theoretical studies on aluminum trialkoxide-initiated lactone ring-opening polymerizations: Roles of alkoxide substituent and monomer ring structure. Comput. Theor. Chem. 2016, 1097, 25-32. (IF: 1.403)

# 2. การนำผลงานวิจัยไปใช้ประโยชน์

- เชิงวิชาการ (มีการพัฒนาการเรียนการสอน/สร้างนักวิจัยใหม่)

ผลการดำเนินงานโครงการ "การประยุกต์ใช้คอมพิวเตอร์ช่วย วิศวกรรมเอนไซม์ฟรุกโตซิลทรานเฟอเรสตระกูล 32 เพื่อใช้ในการสังเคราะห์ ฟรุกโตโอลิโกแซคคาไรด์" ได้สร้างองค์ความรู้ใหม่ต่อวงการวิชาการ โดย สามารถทำนายกระบวนการย่อยสลายและย้ายหมู่ฟรุกโตสในระดับโมเลกุล และอธิบายผลการทดลองก่อนหน้านี้ ว่าทำไมกระบวนการทั้งสองจึงเกิดขึ้นได้

ในเอนไซม์ฟรุกโตซิลทรานเฟอเรส ทั้ง ๆ ที่โดยทั่วไปกระบวนการย่อยสลาย เป็นกระบวนการที่พบได้เป็นส่วนใหญ่ในกลุ่มเอนไซม์ไกลโคสิเดส นอกจากนี้ ยังสามารถบอกบทบาทของกรดอะมิโนที่เกี่ยวข้องได้ ผลลัพธ์ที่ได้ยังเป็น ประโยชน์ต่อการศึกษาวิศวกรรมโปรตีนเพื่อปรับปรุงสมบัติของเอนไซม์ต่อไป นอกจากนี้ยังมีผลงานวิจัยอื่น ๆ ที่เกิดจากการสะสมความรู้ของโครงการวิจัยไป ใช้ต่อยอดกับระบบทางเคมีที่สำคัญ ๆ ได้ เช่น การออกแบบตัวเร่งปฏิกิริยาพอลิ เมอร์ไรเซชันแบบเปิดวง การทำนายตำแหน่งยึดเกาะของสารยับยั้งที่บริเวณเร่ง ของโปรตีนเป้าหมาย เป็นต้น

โดยสรุปผลการดำเนินโครงการในช่วงระยะเวลา 2 ปี ผู้วิจัย สามารถตีพิมพ์บทความวิจัยในระดับนานาชาติที่มีค่า impact factor ไปแล้ว จำนวน 3 เรื่อง และกำลังรอตีพิมพ์ อีก 1 เรื่อง โดยมีการนำผลงานวิจัยไป เผยแพร่ในงานประชุมวิชาการระดับนานาชาติ งานสัมมนา รวมไปถึงการนำไป บูรณาการกับการเรียนการสอนในรายวิชา 242413 เคมีคำนวณเบื้องตัน และ 256449 งานวิจัยแนวใหม่ทางเคมีเชิงฟิสิกส์ ของคณะวิทยาศาสตร์ มหาวิทยาลัยพะเยา ในด้านพัฒนาคน งานวิจัยและความรู้ที่เกิดขึ้น ยังถูก ถ่ายทอดไปยังนักเรียนระดับมัธยมศึกษาตอนปลายในโครงการ วมว. โรงเรียน สาธิตมหาวิทยาลัยพะเยา ซึ่งจะเติบโตเป็นนักวิจัยในอนาคตต่อไป

- 3. อื่นๆ (เช่น ผลงานตีพิมพ์ในวารสารวิชาการในประเทศ การเสนอผลงานในที่ประชุม วิชาการ หนังสือ การจดสิทธิบัตร)
  - 3.1 การเสนอผลงาน/เข้าร่วมในที่ประชุมวิชาการ
    - 1. **Jitonnom J.**, Mulholland, A.J., James R. Ketudat Cairns, Hannongbua, S., "Modeling of Hydrolysis and Transglycosylation in Glycosidases: Insights from QM/MM and QM Cluster Approaches", the 8th International Theoretical Biophysics Symposium (THEOBIO 2017) at Donostia/San Sebastian in Spain, 26-30 June 2017.
    - 2. **Jitonnom J**., Mulholland, A.J., James R. Ketudat Cairns, Hannongbua, S., "Modeling of Hydrolysis and Transglycosylation in Glycosidases: Insights from QM/MM and QM Cluster Approaches", "นักวิจัยรุ่นใหม่...พบ...เมธีวิจัยอาวุโส สกว." ครั้งที่ 16 ระหว่างวันพุธที่ 11 วันศุกร์ที่ 13 มกราคม พ.ศ. 2560 ณ โรงแรมเดอะรีเจ้นท์ ชะอำ บีช รีสอร์ท จังหวัดเพชรบุรี.

Reprint of the 3 published papers

- 1. **Jitonnom J.**, Meelua W. Effect of ligand structure in the trimethylene carbonate polymerization by cationic zirconocene catalysts: A "naked model" DFT study. **J. Organometal. Chem.**, 2017, 841, 48-56.
- 2. **Jitonnom J.**, Meelua W. Cationic ring-opening polymerization of cyclic carbonates and lactones by group 4 metallocenes: A theoretical study on mechanism and ring-strain effects. **J. Theor. Comput. Chem.**, 2017, 16, 1750003.
- 3. **Jitonnom J.**, Molloy R., Punyodom W., Meelua W. Theoretical studies on aluminum trialkoxide-initiated lactone ring-opening polymerizations: Roles of alkoxide substituent and monomer ring structure. **Comput. Theor. Chem.**, 2016, 1097, 25-32.